

Managing Systematic Errors in Ice Crystal Growth Experiments

Kenneth G. Libbrecht

Department of Physics, California Institute of Technology
Pasadena, California 91125

Abstract: We describe how surface interactions can affect the growth of ice crystal facets in contact with a substrate by lowering the normal nucleation barrier on the ice surface. We also describe how the resulting enhanced growth rates can produce systematic errors even when measuring the growth of facets not contacting the substrate. From an analysis of the diffusion dynamics we then develop a simple procedure for approximately correcting ice growth data, thus substantially reducing these systematic errors. We have found this technique to be quite useful for interpreting ice growth data and extracting the intrinsic attachment coefficients of ice surfaces.

1 Introduction

We recently developed a new experimental apparatus for making precise measurements of the growth rates of ice facet surfaces as a function of temperature and supersaturation [1, 2]. During the course of our investigations, we found that interactions with our sapphire substrate introduced systematic errors that could be substantial in some circumstances. In particular, we found that ice facets that were in contact with the substrate tended to grow faster than otherwise expected, in a variable and somewhat unpredictable fashion. This enhanced growth from substrate interactions was particularly evident at low supersaturations.

We believe that the enhanced growth arises because the ice/substrate interaction creates molecular steps on the intersecting ice surface, thus lowering the normal nucleation barrier that is present on an ice facet. A contact-angle model is sufficient to explain these observations, as illustrated in Figure 1. If the ice/substrate contact angle θ_{contact} is less than the intersection angle θ_{facet} between the facet and the substrate, then the ice/substrate contact will act as a source of molecular steps on the ice facet, as seen in the left diagram in Figure 1. The presence of these molecular steps then reduces the normal nucleation barrier on the ice facet, and the growth enhancement will be most pronounced at low supersaturation, when the normal facet growth rate is especially low.

If $\theta_{\text{contact}} > \theta_{\text{facet}}$, however, then the contact will not be a source of steps, and there will be no enhanced growth arising from substrate interactions, as seen in the right diagram in Figure 1. Since θ_{contact} depends on the chemical nature of the substrate, as well as on any chemical residue on an imperfectly cleaned substrate, we found that the ice growth behavior from substrate interactions can be somewhat unpredictable.

This same effect appears to have affected other ice growth experiments reported in the literature. For example, in [3] the authors found that prism facets not intersecting their substrate (facet type P in their paper) grew approximately five times slower than facets that did intersect the substrate, even while the facets were all exposed to essentially the same growth conditions. Also, in [4] the authors found that facets in contact with the exterior of their capillary tubes grew more quickly than other facets, and that contact with the foreign surface also reduced the measured nucleation

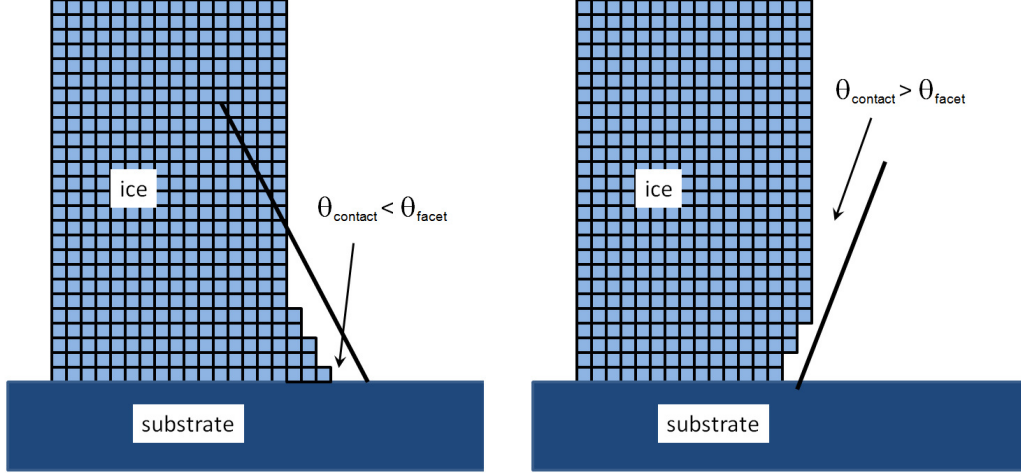


Figure 1: An ice crystal resting on a substrate with $\theta_{facet} = 90$ degrees, which is the case when the basal facet of a hexagonal prism rests on the substrate. At left $\theta_{contact} < \theta_{facet}$, so substrate interactions introduce molecular steps on the intersecting facet surface, thus reducing the nucleation barrier that normally inhibits crystal growth on that surface. At right $\theta_{contact} > \theta_{facet}$ and the nucleation barrier is not affected.

barrier. Qualitatively the effects described in these two experiments agreed with our observations, suggesting that all three experiments were witnessing essentially the same phenomenon.

In addition, we found that substrate interactions can substantially influence the growth of neighboring ice facets that are not directly in contact with the substrate. The mechanism is that rapid growth of the contacting facets lowers the supersaturation field around the crystal, owing to particle diffusion through the background gas, and this reduces the growth rates of the neighboring facets. This effect is very large for background pressures near one bar, but even at 10-20 mbar (typical of our measurements) it can introduce significant systematic errors. In addition, as we see below, the effects can be important for measurements made both at low and high supersaturations.

The remainder of this paper presents: 1) a detailed analysis of how substrate interactions affect the growth rates of neighboring crystal facets, those not in contact with the substrate; and 2) a method for modeling and approximately correcting for substrate interactions.

2 Systematic Errors from Substrate Interactions

Our first, rather obvious, conclusion from these observations is that growth measurements of ice facet surfaces in contact with a substrate may yield little useful information on the intrinsic ice growth rates. A faceted surface typically implies a nucleation barrier, and any reduction of that barrier from substrate interactions likely produces unacceptably large systematic errors. Of course, it is possible that substrate interactions are negligible in some circumstances, but it rests on the experimenter to convincingly demonstrate that this is the case.

We tried to find a suitable superhydrophobic coating for our sapphire substrate that would increase $\theta_{contact}$ and thus reduce the effects of substrate interactions, as shown in Figure 1. To date we have not found a surface treatment that is superior to a very clean sapphire surface, but much research effort is currently being spent on developing superhydrophobic coatings for a range of materials. We believe that future measurements would likely benefit from finding suitable superhydrophobic surface treatments.

Our second conclusion is that the indirect effects on neighboring facets can be quite important also, even at low background pressures. Some diffusion modeling is required to understand the magnitude of these effects on ice crystal growth experiments. The remainder of this paper is focused on outlining the diffusion modeling of this problem and developing a strategy for managing and correcting the resulting systematic errors in experimental data.

To develop a quantitative diffusion model, the present discussion considers the problem of crystal growth in the presence of an inert background gas, in which the transport of water vapor is governed by simple diffusion through the gas background. We further simplify to the isothermal case, which is a reasonably accurate approximation for growth on a substrate, since the substrate acts as a thermal reservoir that readily absorbs the latent heat generated from crystal growth [5].

2.1 The Hemispherical Case with no Substrate Interactions

To set the notation and basic scales in the problem, we first examine the case of a hemispherical crystal of radius R growing on an infinite substrate. We assume a constant supersaturation σ_∞ far from the crystal and assume a single condensation coefficient $\alpha(\sigma)$ for the crystal surface. The diffusion equation and boundary conditions for this problem are equivalent to the spherical case, which can be solved analytically. Following the notation in [5], the growth rate of the crystal surface is

$$\begin{aligned} v &= \alpha_{surf} v_{kin} \sigma_{surf} \\ &= \frac{c_{sat}}{c_{solid}} D \frac{d\sigma}{dR} \Big|_{surf} \end{aligned}$$

where $\alpha_{surf} = \alpha(\sigma_{surf})$ is the condensation coefficient at the ice surface and $\sigma_{surf} = \sigma(R)$. The diffusion equation together with these mixed boundary conditions for $\sigma(r)$ give the solution [5]

$$v = \frac{\alpha_{surf} \alpha_{diff}}{\alpha_{surf} + \alpha_{diff}} v_{kin} \sigma_\infty$$

where

$$\begin{aligned} \alpha_{diff} &= \frac{c_{sat} D}{c_{solid} v_{kin} R} = \frac{D}{R} \sqrt{\frac{2\pi m}{kT}} \\ &\approx 0.15 \left(\frac{1 \mu\text{m}}{R} \right) \left(\frac{D}{D_{air}} \right) \end{aligned} \tag{1}$$

where D is the diffusion constant in the background gas. For the final expression we used $D_{air} = 2 \times 10^{-5} \text{ m}^2/\text{sec}$ for the diffusion constant of water vapor in air at a pressure of one bar. To a good approximation D is inversely proportional to the background gas pressure.

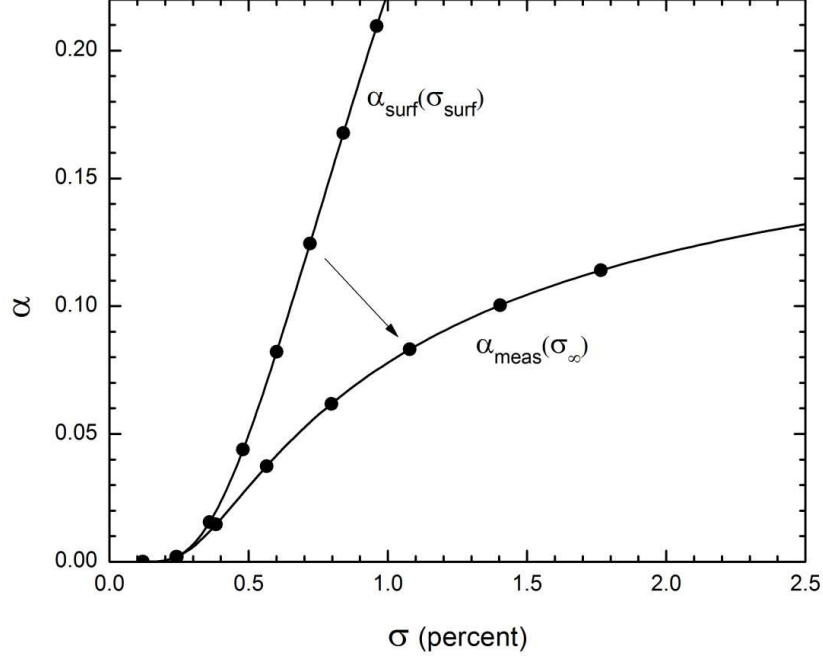


Figure 2: Calculated plots of the functions $\alpha_{surf}(\sigma_{surf})$ and $\alpha_{meas}(\sigma_{\infty})$ defined in the text, for the case of a hemispherical crystal growing on a substrate. The individual points show the correspondence between the two curves. Here we used $\alpha_{diff} = 0.25$, corresponding to a crystal radius of $R \approx 30 \mu\text{m}$ in a background pressure of 20 mbar (both typical of our measurements), and an intrinsic attachment coefficient of $\alpha_{surf}(\sigma_{surf}) = \exp(-0.015/\sigma_{surf})$ (typical for basal facet growth at temperatures near -13 C) [2].

From the analytic solution we also have the supersaturation at the ice surface

$$\sigma_{surf} = \frac{\alpha_{diff}}{\alpha_{surf} + \alpha_{diff}} \sigma_{\infty} \quad (2)$$

and eliminating α_{surf} from this expression gives

$$\sigma_{surf} = \sigma_{\infty} - \frac{v}{\alpha_{diff} v_{kin}} \quad (3)$$

which is exact for the spherical and hemispherical cases.

When measuring ice crystal growth rates [1, 2], we typically establish a supersaturation σ_{∞} far from the crystal and then measure the crystal dimensions as a function of time and σ_{∞} , with the goal of extracting the intrinsic attachment coefficient $\alpha(\sigma_{surf})$ for the growing surfaces. In the limit of fast diffusion (or slow attachment kinetics), $\alpha_{surf} \ll \alpha_{diff}$ and the hemispherical case gives

$$\alpha_{surf} \approx \alpha_{meas} = \frac{v}{v_{kin} \sigma_{\infty}} \quad (4)$$

which defines the measured quantity α_{meas} . If diffusion cannot be neglected, then

$$\alpha_{meas} = \frac{\alpha_{surf}\alpha_{diff}}{\alpha_{surf} + \alpha_{diff}} \quad (5)$$

and a plot of $\alpha_{meas}(\sigma_\infty)$ typically deviates from the desired $\alpha_{surf}(\sigma_{surf})$ at high σ_∞ . An example of this is shown in Figure 2, and plots of $\alpha_{meas}(\sigma_\infty)$ from our data show this same functional form [1, 2].

The example in Figure 2 shows that $\alpha_{meas}(\sigma_\infty)$ is approximately equal to $\alpha_{surf}(\sigma_{surf})$ at low supersaturations, which is precisely when $\alpha_{surf} \ll \alpha_{diff}$. Increasing σ_∞ increases σ_{surf} until $\alpha_{surf}(\sigma_{surf})$ becomes larger and the criterion $\alpha_{surf} \ll \alpha_{diff}$ is no longer satisfied. When this occurs, the two curves in Figure 2 deviate from one another.

2.1.1 Correcting the Hemispherical Case

In our experiments we determine σ_∞ and measure the growth velocity v of a facet not contacting the substrate, and from Equation 4 we derive $\alpha_{meas}(\sigma_\infty)$ entirely from measured quantities. Our goal, however, is to determine the intrinsic condensation coefficient $\alpha_{surf}(\sigma_{surf})$. For our idealized hemispherical crystal, we could apply a correction to the data that transforms $\alpha_{meas}(\sigma_\infty)$ into $\alpha_{surf}(\sigma_{surf})$ using

$$\begin{aligned} \sigma_{surf} &= \left(1 - \frac{\alpha_{meas}}{\alpha_{diff}}\right) \sigma_\infty \\ \alpha_{surf}(\sigma_{surf}) &= \left(1 - \frac{\alpha_{meas}}{\alpha_{diff}}\right)^{-1} \alpha_{meas} \end{aligned} \quad (6)$$

where α_{diff} is derived from the measured crystal radius using Equation 1. Clearly this correction works best when $\alpha_{meas} \ll \alpha_{diff}$, or equivalently $\alpha_{surf} \ll \alpha_{diff}$. As long as the crystal growth is limited mainly by attachment kinetics and not by diffusion, then we can use this correction to reasonably extract $\alpha_{surf}(\sigma_{surf})$ from the measured $\alpha_{meas}(\sigma_\infty)$.

2.2 Plate Growth with Substrate Interactions

We next consider the growth of simple hexagonal plate crystals, which is what we observed in [2]. In this case one basal facet is resting on the substrate, and we measure the growth of the opposite basal facet along with the growth of the six prism facets. We typically have $v_{basal} \neq v_{prism}$, and there is no analytic solution of the diffusion equation that gives the supersaturation field $\sigma(x)$ around the crystal.

To see the problems that result, consider the example shown in Figure 3, in which we examine the basal growth of a plate of radius $R \approx 30 \mu\text{m}$ and thickness $H \approx 4 \mu\text{m}$, again at a pressure of 20 mbar. If it so happens that $\alpha_{prism}(\sigma) = \alpha_{basal}(\sigma)$, then $v_{prism} \approx v_{basal}$ and we see that the resulting $\alpha_{meas}(\sigma_\infty)$ looks quite similar to the hemispherical case in Figure 2, with some α_{diff} appropriate for the crystal size and geometry. In particular, we see that $\alpha_{meas}(\sigma_\infty) \approx \alpha_{surf}(\sigma_{surf})$ at low supersaturations, as we saw with the hemispherical case.

If we increase the prism growth rate, however, in this example by setting $\alpha_{prism} = 1$, then the faster prism growth pulls down the supersaturation around the entire crystal. Because $\alpha_{basal}(\sigma)$ is a strong function of σ , this means that the measured basal growth rates are substantially reduced.

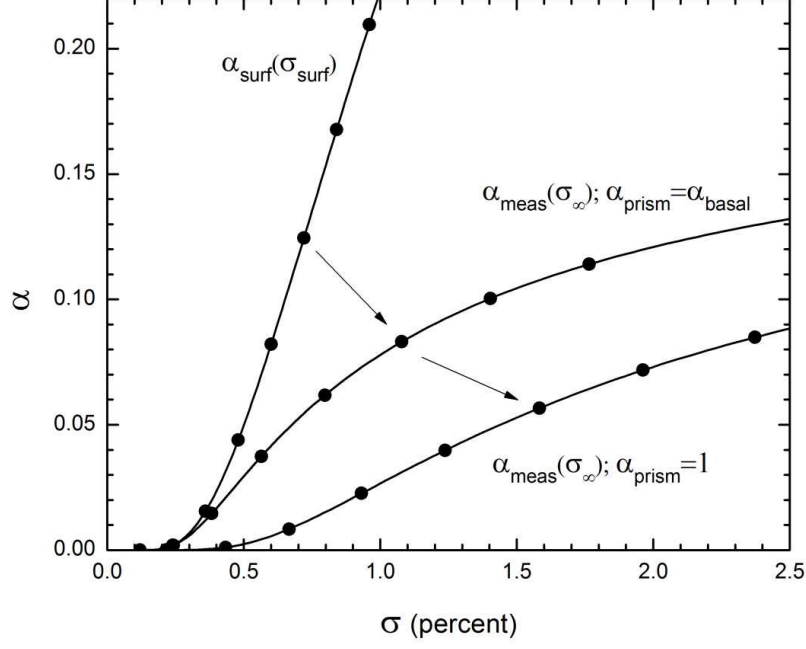


Figure 3: Calculated plots of the functions $\alpha_{surf}(\sigma_{surf})$ and $\alpha_{meas}(\sigma_{\infty})$ for growth of the top basal surface of a hexagonal plate crystal, with the lower basal surface resting on the substrate. The individual points show the correspondence between the three curves. In this example we used the model of a circular disk crystal of radius $R \approx 30 \mu\text{m}$ and thickness $H \approx 4 \mu\text{m}$ in a background pressure of 20 mbar, with the intrinsic basal attachment coefficient $\alpha_{basal} = \alpha_{surf}(\sigma_{surf}) = \exp(-0.015/\sigma_{surf})$. For the middle curve we used $\alpha_{prism} = \alpha_{basal}$, which gives $v_{prism} \approx v_{basal}$ and an $\alpha_{meas}(\sigma_{\infty})$ curve that is similar to that shown in Figure 2. For the lower curve we used $\alpha_{prism} = 1$, giving $v_{prism} > v_{basal}$ and an $\alpha_{meas}(\sigma_{\infty})$ curve that is substantially distorted, especially at low σ_{∞} .

Furthermore, the reduction factor is especially large at low supersaturations, as can be seen by examining the curves in Figure 3. Now this is a rather extreme case, with exceptionally fast prism growth, but it demonstrates how the measured $\alpha_{meas}(\sigma_{\infty})$ can be distorted at both high and low σ_{∞} by diffusion effects, even at quite low background air pressures. These effects can make it difficult to reliably determine $\alpha_{surf}(\sigma_{surf})$ from the measurements, requiring diffusion modeling.

2.2.1 Correcting Experimental Data

In principle one could use numerical modeling of particle diffusion to extract $\alpha_{surf}(\sigma_{surf})$ from $\alpha_{meas}(\sigma_{\infty})$, provided the difference is not too large. In practice, however, such modeling is quite computationally intensive, and it is problematic to do a detailed numerical model for each of hundreds of test crystals. We would therefore like a simpler analytic approach that would allow us to apply a rough correction to our data. To produce such an approximate correction, we generalize Equation

3 by writing

$$\sigma_{surf} \approx \sigma_{corr} = \sigma_{\infty} - \sum_i \frac{f_i v_i}{\alpha_{diff,eff} v_{kin}} \quad (7)$$

where the sum is over the different growing regions of the crystal (in this case the one basal facet and six prism facets). The f_i give the fractional areas of the different regions (with $\sum f_i = 1$), where each region is growing with velocity v_i . From Equation 1 we take

$$\alpha_{diff,eff} \approx 0.15 \left(\frac{1 \text{ } \mu\text{m}}{R_{eff}} \right) \left(\frac{D}{D_{air}} \right)$$

where

$$2\pi R_{eff}^2 = \sum_i A_i$$

and the A_i give the areas of each crystal region. Note that Equation 7 is exact for the hemispherical case, where it reduces to Equation 3. For the facet of interest we then have

$$\alpha_{surf}(\sigma_{surf}) \approx \frac{v}{v_{kin} \sigma_{surf}} \approx \frac{\sigma_{\infty}}{\sigma_{corr}} \alpha_{meas}$$

and this correction can be applied to each data point.

A key feature in this correction is that the v_i , A_i , and f_i can all be extracted from the measured crystal size and geometry as a function of time. If the prism growth is influenced by substrate interactions, as we describe above, we can still use this formalism to correct for changes in the supersaturation field that affect the basal growth measurements. As long as the difference $\sigma_{\infty} - \sigma_{corr}$ is not too great, we can determine $\alpha_{surf}(\sigma_{surf})$ for the basal surface.

Figure 4 shows how this correction process works in practice, using a plate-like crystal growing at a temperature of -12 C, taken from [2]. Note that the prism growth rate at the beginning of this measurement was $v_{prism} \approx 63$ nm/sec, when $\sigma_{\infty} \approx 0.33\%$. If α_{prism} had been equal to unity, as we assumed in the example in Figure 3, then the radial growth would have been a much faster $v_{prism} \approx 900$ nm/sec. Thus we verify that the $\alpha_{prism} = 1$ case in Figure 3 was somewhat extreme, and in our actual data the corrections are usually substantially smaller.

Note also that our fit to the uncorrected data in Figure 4 gave $\alpha_{diff} = 0.09$, a value roughly a factor of two smaller than the α_{diff} calculated from the size and geometry of the crystal. We observed this discrepancy frequently in our basal growth data, and we find it is nicely resolved by applying the above data correction. The corrected data give a significantly better measure of the intrinsic attachment coefficient $\alpha_{surf}(\sigma_{surf})$, with reduced systematic effects compared with using only the uncorrected $\alpha_{meas}(\sigma_{\infty})$. This improvement is accompanied by only a modest increase in the scatter of the data points arising from the imperfect correction process.

It is straightforward as well to apply this same correction process to measurements of prism facet growth, where one prism facet rests on the substrate. The area factors f_i must be changed to fit the prism growth case, but otherwise the prism growth correction is identical to the basal case described above.

3 Conclusion

The approximate correction described above serves several purposes in the analysis of our data: 1) it reduces the systematic errors in our determination of $\alpha_{surf}(\sigma_{surf})$ for the growth of facets that

do not contact the substrate; 2) it eliminates the fit parameter α_{diff} when fitting the observed $\alpha_{meas}(\sigma_\infty)$ (see [2]); 3) a comparison of $\alpha_{meas}(\sigma_\infty)$ and $\alpha_{surf}(\sigma_{surf})$ indicates which crystals have large correction factors and thus should be given less weight in determining $\alpha_{surf}(\sigma_{surf})$; and 4) the correction allows us to make reliable measurements of $\alpha_{surf}(\sigma_{surf})$ over a broader range of experimental conditions than we could without the data correction.

Although the correction is only approximately valid, it nevertheless does an adequate job of reducing an important systematic effect. We have found it to be a valuable tool for interpreting measurements of the growth of ice crystals on substrates at low background pressures.

References

- [1] K. G. Libbrecht, “An improved apparatus for measuring the growth of ice crystals from water vapor,” arXiv:1109.1511 (2011).
- [2] K. G. Libbrecht and M. E. Rickerby, “Measurements of growth rates of (0001) ice crystal surfaces,” arXiv:1110.5828 (2011).
- [3] W. Beckmann, R. Lacmann, and A. Blerfreund, “Growth rates and habits of ice crystals grown from the vapor phase,” J. Phys. Chem 87, 4142-4146 (1983).
- [4] J. Nelson and C. Knight, “Snow crystal habit changes explained by layer nucleation,” J. Atmos. Sci. 55, 1452-1465 (1998).
- [5] K. G. Libbrecht, “The physics of snow crystals,” Rep. Prog. Phys. 68, 855-895 (2005).

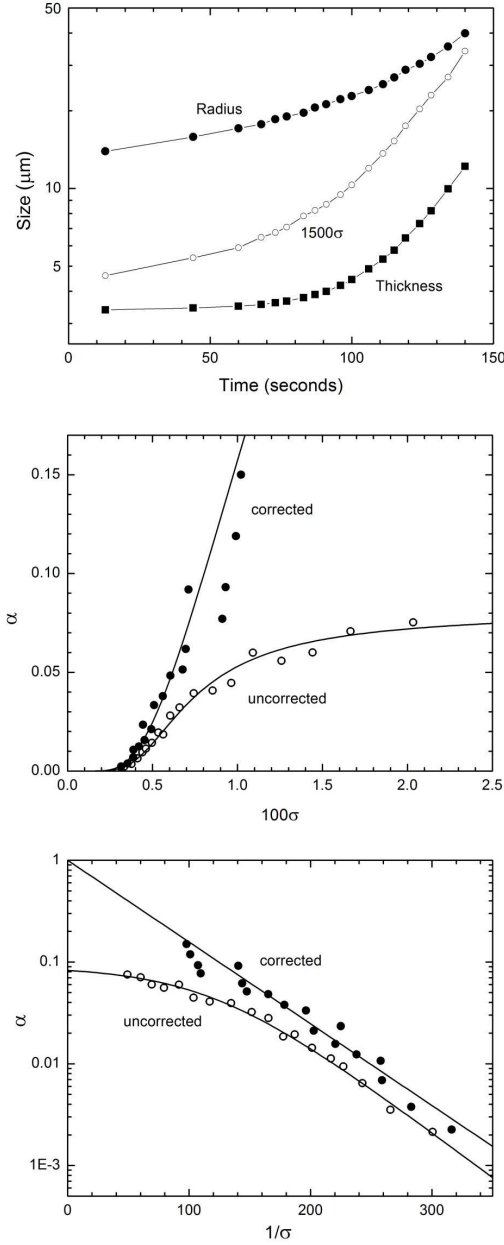


Figure 4: An example of actual ice crystal growth data corrected using the procedure described in the text. (Top) The measured radius and thickness of a hexagonal plate crystal as a function of time during a growth run from [2], along with $1500\sigma_\infty$ (in absolute units). The background pressure during this measurement was 25 mbar. Note that at early times the radius increased more rapidly than the thickness ($v_{prism} > v_{basal}$) because of substrate interactions. (Middle, Bottom) The directly measured condensation coefficient $\alpha_{meas}(\sigma_\infty)$ (open symbols) and the corrected measurement $\alpha(\sigma_{surf})$ (closed symbols). The fit lines in both these plots are $\alpha_{meas}(\sigma_\infty) = \exp(-0.0205/\sigma)\alpha_{diff}/(\exp(-0.0205/\sigma) + \alpha_{diff})$, with $\alpha_{diff} = 0.09$, and $\alpha(\sigma_{surf}) = \exp(-0.0185/\sigma)$.